Herpesvirus entry mediator regulates hypoxia-inducible factor–1α and erythropoiesis in mice

Yukimi Sakoda,[1] Sudarshan Anand,[2] Yuming Zhao,[1] Jang-June Park,[1] Yingjia Liu,[1] Atsuo Kuramasu,[1,3] Nico van Rooijen,[4] Ling Chen,[5] Scott E. Strome,[1,6] Wayne W. Hancock,[7] Lieping Chen,[2] and Koji Tamada[1,3,6]

[1]Marlene and Stewart Greenebaum Cancer Center, University of Maryland, Baltimore, Maryland, USA. [2]Department of Oncology and Institute for Cell Engineering, Johns Hopkins University School of Medicine, Baltimore, Maryland, USA. [3]Yamaguchi University Graduate School of Medicine, Ube, Japan. [4]Department of Molecular Cell Biology, Vrije Universiteit Medical Center, Amsterdam, The Netherlands. [5]Department of Medicine and [6]Department of Otorhinolaryngology-Head and Neck Surgery, University of Maryland, Baltimore, Maryland, USA. [7]Department of Pathology and Laboratory Medicine, University of Pennsylvania, Philadelphia, Pennsylvania, USA.

Erythropoiesis, the production of red blood cells, must be tightly controlled to ensure adequate oxygen delivery to tissues without causing thrombosis or stroke. Control of physiologic and pathologic erythropoiesis is dependent predominantly on erythropoietin (EPO), the expression of which is regulated by hypoxia-inducible factor (HIF) activity in response to low oxygen tension. Accumulating evidence indicates that oxygen-independent mediators, including inflammatory stimuli, cytokines, and growth factors, also upregulate HIF activity, but it is unclear whether these signals also result in EPO production and erythropoiesis in vivo. Here, we found that signaling through herpesvirus entry mediator (HVEM), a molecule of the TNF receptor superfamily, promoted HIF-1α activity in the kidney and subsequently facilitated renal Epo production and erythropoiesis in vivo under normoxic conditions. This Epo upregulation was mediated by increased production of NO by renal macrophages. *Hvem*-deficient mice displayed impaired Epo expression and aggravated anemia in response to erythropoietic stress. These data reveal that HVEM signaling functions to promote HIF-1α activity and Epo production, and thus to regulate erythropoiesis. Furthermore, our findings suggest that this molecular mechanism could represent a therapeutic target for Epo-responsive diseases, including anemia.

Introduction

Erythropoietin (EPO) is a glycoprotein hormone that serves as a primary regulator of differentiation, proliferation, and survival of erythroid progenitor cells (1, 2). In adulthood, EPO is mainly produced by the kidneys, although the liver also serves as a pivotal EPO-producing organ during the fetal stage (3). *EPO* gene expression is promoted by hypoxia-inducible factor (HIF), a transcription regulator composed of α and β subunits (1, 2). There are at least 3 subtypes of the α subunit (HIF-1α–HIF-3α), and HIF-1α and HIF-2α, but not HIF-3α, contain a C-terminal transactivation domain that stimulates *EPO* gene expression (4, 5). Whereas HIF-1β is constantly present in the nucleus, HIF-1α and HIF-2α are generally undetectable because of oxygen-sensitive degradation mechanisms. With sufficient oxygen supply, 2 specific proline residues of HIF-α are hydroxylated by prolyl hydroxylase domain–containing (PHD-containing) enzymes, and HIF-α is therefore recognized by von-Hippel-Lindau protein (pVHL), poly-ubiquitinated, and processed by proteasomal degradation (6–8). In addition, transcriptional activity of HIF is suppressed by factor inhibiting HIF (FIH) in normoxic condition, as FIH induces hydroxylation of an asparagine residue of HIF-α and thus prevents HIF-α from interacting with p300 transcriptional coactivator (9). Under hypoxic conditions, on the other hand, enzymatic activity of PHD and FIH are suppressed, so that HIF-α is stabilized and transcriptional activity of HIF-α/β dimers is upregulated. As a result, expression of *EPO* and other genes under HIF transcriptional control is augmented.

Recent studies have provided compelling evidence that various factors other than oxygen concentration also promote HIF activity, including inflammatory stimuli, cytokines, hormones, and growth factors (10, 11). In inflammatory conditions, NF-κB plays a crucial role in induction of *Hif1*α transcription, as deficiency of the *IKK*β gene attenuates *Hif1*α mRNA expression in bacterial infection or LPS stimulation (12). Cytokines and growth factors activate signals through PI3K/AKT/mTOR and MAPK, which increase HIF-1α protein synthesis (13, 14). NO stabilizes HIF-1α protein by inhibiting PHD activity and by inducing HIF-1α S-nitrosylation, while it also activates HIF-1α by triggering PI3K and MAPK signaling pathways (15–18). Despite these accumulating data, the functions of oxygen-independent HIF-1α stimulation in vivo are largely unknown. It is of particular interest whether oxygen-independent HIF-1α activation upregulates EPO expression and subsequently facilitates erythropoiesis in vivo. Addressing this question holds significance in order to delineate the entire view of erythropoietic homeostasis and to explore novel therapeutic approaches to treat EPO-responsive diseases.

Herpesvirus entry mediator (HVEM), a cell surface molecule belonging to the TNF receptor superfamily, is ubiquitously expressed on immune cells of both myeloid and lymphoid lineages (19). HVEM signaling recruits TNF receptor–associated factor 1 (TRAF1), TRAF2, TRAF3, and TRAF5, leading to activation of NF-κB and JNK/AP-1 signaling pathways (20, 21). In the immune system, HVEM on T cells serves as a potent costimulatory receptor and induces Th1-type cytokine production (22, 23). HVEM signaling in neutrophils and macrophages promotes their expression of NO and reactive oxygen species (24). In the present study, using a mouse model, we found that HVEM signaling upregulated renal Epo expression and subse-

Authorship note: Yukimi Sakoda, Sudarshan Anand, and Yuming Zhao contributed equally to this work.

Conflict of interest: Scott E. Strome receives royalties through the Mayo Clinic College of Medicine for intellectual property related to B7-H1 and 4-1BB. He is also a cofounder and major stockholder in Gliknik Inc., a biotechnology company.

Citation for this article: *J Clin Invest.* 2011;121(12):4810–4819. doi:10.1172/JCI57332.

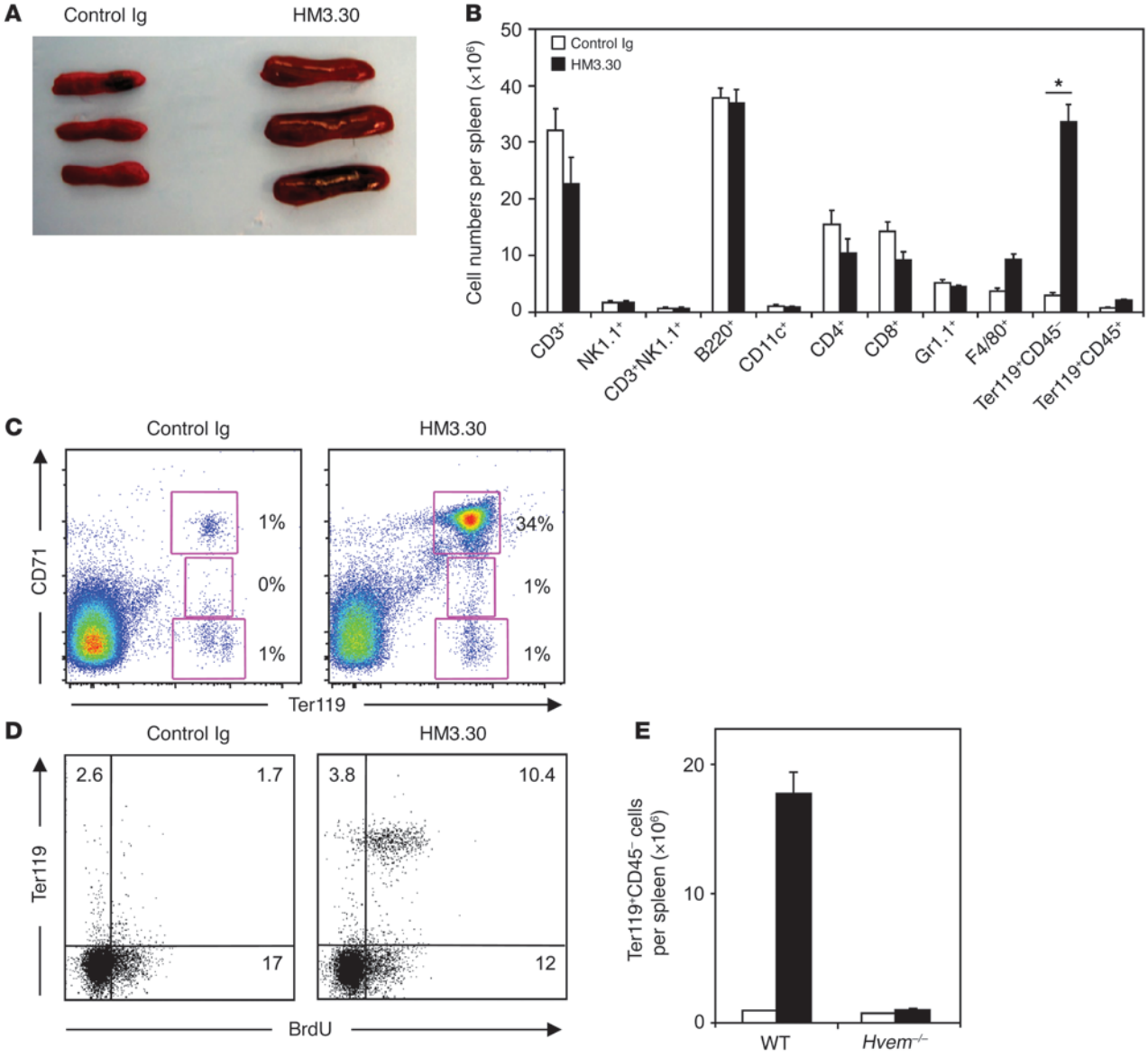

Figure 1
Administration of the anti-HVEM mAb HM3.30 induces erythropoiesis in mice. (**A**–**D**) WT C57BL/6 mice were injected i.p. with 150 μg control Ig or HM3.30 and examined on day 4. (**A**) Gross appearance of the treated spleen. (**B**) Absolute numbers of the indicated cell populations per spleen in mice treated with control Ig or HM3.30, examined by flow cytometry ($n \geq 5$). *$P < 0.01$. (**C**) Percent basophilic (Ter119$^+$CD71^{hi}), polychromatophilic (Ter119$^+$CD71^{med}), and orthochromatic (Ter119$^+$CD71^{lo}) erythroblasts in spleen, examined by flow cytometry. (**D**) In addition to Ab injection, mice were treated i.p. with 100 μg BrdU every 24 hours. Spleen cells were analyzed for Ter119 and BrdU staining by flow cytometry. Numbers denote the percentage of cells in the respective gates. (**E**) Absolute number of Ter119$^+$CD45$^-$ erythrocytes in the spleen of mice treated with control Ig or HM3.30 as in **A**–**C** ($n = 3$ each). Data represent mean ± SD.

quent erythropoiesis in vivo under normoxic conditions via NO production by macrophages and HIF-1α activation in the kidney. These results reveal a biological function of HVEM in HIF-1α/Epo regulation and erythropoiesis, a finding we believe to be novel.

Results

Agonistic mAb against HVEM induces erythropoiesis in vivo. We previously reported that HVEM delivers potent costimulatory signals in T cells (22, 23). To investigate the role of HVEM in antitumor immunotherapy, we generated an anti-HVEM mAb clone, HM3.30, which has an agonistic potential (Supplemental Figure 1; supplemental material available online with this article; doi:10.1172/JCI57332DS1). When we injected HM3.30 in vivo to examine antitumor effects, we unexpectedly observed splenomegaly in the treated mice (Figure 1A). Surprisingly, upon examination of hematopoietic lineages, we found that the HM3.30-induced splenomegaly was associated with a greater than 10-fold increase of Ter119$^+$CD45$^-$ erythroid progenitor cells (Figure 1B). Besides Ter119$^+$ cells, HM3.30 induced a slight (approximately 2-fold) increase of F4/80$^+$ cells, while no significant changes

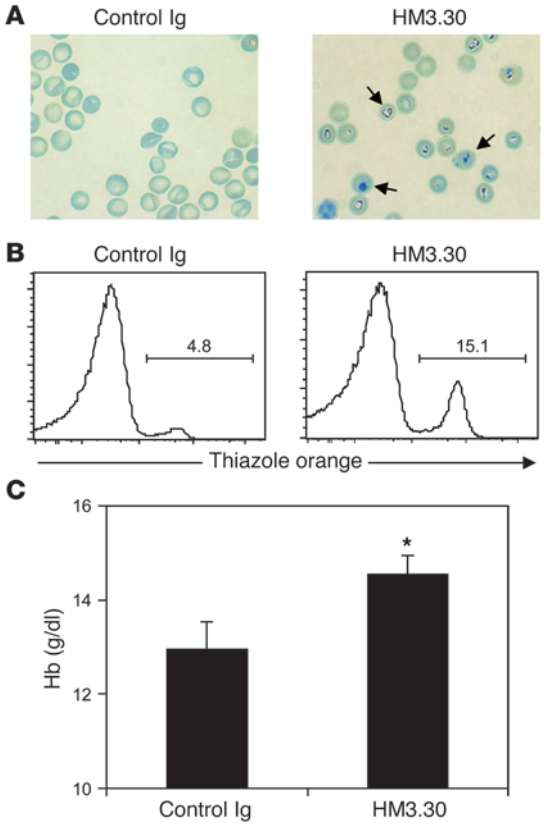

Figure 2
HM3.30 treatment induces erythropoiesis in peripheral blood. (**A** and **B**) WT mice were injected i.p. with 150 μg control Ig or HM3.30 and examined after 4 days. (**A**) Peripheral blood smears were prepared and stained by new methylene blue. Typical staining of residual RNA in reticulocytes is denoted by arrows. Representative images from at least 20 examined fields are shown. Original magnification, ×400. (**B**) Percent reticulocytes in PBMCs, assessed by flow cytometry using thiazole orange stain. Data are representative of 3 independently repeated experiments. Numbers denote the percentage of reticulocytes positively stained with thiazole orange in PBMCs. (**C**) *Rag*$^{-/-}$ mice were injected i.p. with 150 μg control Ig or HM3.30 on days 0, 5, 10, and 15 (n = 3 per group). On day 16, peripheral blood Hb level was measured. Data represent mean ± SD. *P < 0.05.

in other hematopoietic lineages were observed. The increased erythroid progenitor cells predominantly consisted of Ter119^{+}CD71^{hi} basophilic erythroblasts, which underwent proliferation, as shown by active uptake of BrdU (Figure 1, C and D). When HM3.30 was injected into *Hvem*$^{-/-}$ mice, the increase of erythroid lineage cells was completely abolished (Figure 1E), which indicates that these effects are specific to HM3.30 interaction with HVEM. The effect of HM3.30 was associated with its agonistic feature, since LBH1, an antagonistic but not agonistic anti-HVEM mAb (25), showed little effect on erythropoiesis (Supplemental Figure 2).

The effect of HM3.30 in erythropoiesis was also observed in peripheral blood. A significant increase in reticulocytes was detected after HM3.30 injection by smear stained with new methylene blue and by flow cytometric analysis with thiazole orange staining (Figure 2, A and B). In addition, repetitive injections of HM3.30 resulted in a significant increase of hemoglobin (Hb) level in the peripheral blood (control Ig, 12.9 ± 0.58 g/dl; HM3.30, 14.5 ± 0.38 g/dl; P < 0.05; Figure 2C). Complete blood count analysis revealed that HM3.30 administration increased Hb, red blood cell number, and hematocrit, but did not induce changes in other values, including MCV, MCH, MCHC, platelet number, and total and differential white blood cell counts (data not shown). Taken in concert, these results indicate that in vivo stimulation of HVEM by an agonistic mAb induces selective erythropoiesis.

Role of BM in HVEM-mediated erythropoiesis. We next sought to determine the organs responsible for the erythropoiesis mediated by HVEM signaling. Specifically, it was unclear whether HM3.30 stimulates erythroid progenitor cells in the BM or triggers erythropoiesis in extramedullary sites, such as the spleen. To address this question, we first analyzed the kinetics of erythrocytosis in the BM, spleen, and peripheral blood after HM3.30 injection. The increase in Ter119^{+} erythroid cells peaked at days 2 and 4 in the BM, day 4 in the spleen, and after day 6 in PBMCs (Figure 3A). Based on this observation, we postulated that HVEM-mediated erythropoiesis originates from the BM. Consistent with this notion, the benzidine-positive erythrocyte CFU (CFU-E) number significantly increased in the culture of BM cells of HM3.30-treated mice compared with that of control Ig–treated mice (Figure 3B). In addition, erythropoiesis in BM and PBMCs induced by HM3.30 injection remained intact, even in splenectomized mice (Figure 3C). Taken together, these results suggest an important role of BM progenitor cells in HVEM-mediated erythropoiesis, although supportive functions of non-BM organs remain possible.

HVEM signals upregulate renal production of Epo. To account for the robust expansion of BM progenitor cells of erythroid lineage, we hypothesized that HVEM signals mediate their effects by inducing Epo production. When serum Epo levels were measured after HM3.30 injection, we indeed detected a significant increase in Epo, peaking 16 hours after injection and then gradually decreasing over the next 7 days (Figure 4A). The HVEM-induced erythropoiesis was markedly, but not fully, attenuated by coadministration of anti-Epo neutralizing Ab (Figure 4B), indicative of a causative role of Epo. Although Epo is predominantly expressed in the kidneys in adult mice, it can be also produced by the liver under various conditions (26, 27). To determine the origin of Epo induced by HVEM signals, we examined *Epo* mRNA levels in the kidney and liver by real-time PCR. HM3.30 injection substantially increased *Epo* mRNA in the kidney, but not in the liver (Figure 4C). Removal of the kidneys completely abrogated HM3.30-induced Epo upregulation (Figure 4D), providing compelling evidence that HVEM signaling facilitates Epo production in the kidneys.

Since the effects of HM3.30 mAb were associated with its agonistic features, we next examined whether loss of HVEM inversely diminishes Epo production and causes anemia. In a steady-state condition, *Hvem*$^{-/-}$ mice expressed normal levels of serum Epo and did not demonstrate anemia (data not shown). On the other hand, in response to erythropoietic stress induced by cisplatin administration, *Hvem*$^{-/-}$ mice showed significantly lower serum Epo responses than did WT mice (Figure 4E) and suffered from aggravated anemia (WT, 13.0 ± 0.59 g/dl, *Hvem*$^{-/-}$, 11.3 ± 0.24 g/dl; P < 0.05; Figure 4F). These results indicate that endogenous HVEM signaling plays an important role in the induction and/or maintenance of optimal Epo levels in vivo, and therefore in prevention and recovery from anemia.

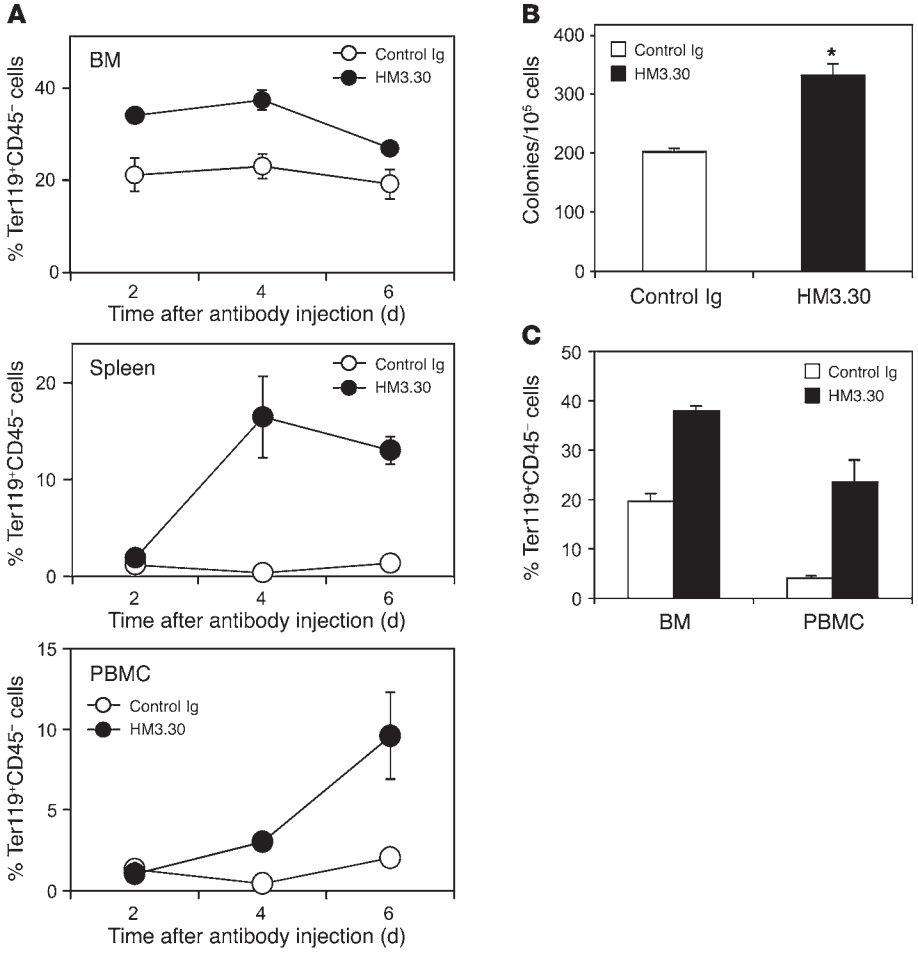

Figure 3
HM3.30 treatment promotes erythropoiesis independent of spleen. (**A**) WT mice were injected i.p. with 150 μg control Ig or HM3.30. After 2, 4, and 6 days, percent Ter119$^+$CD45$^-$ cells in BM, spleen, and PBMCs was measured by flow cytometry. (**B**) WT mice were treated as in **A**; 1 day later, BM cells were harvested and 2 × 10^5 cells were cultured in the methylcellulose media for CFU-E assay. After 2 days, the number of colonies was counted by benzidine staining. *$P < 0.05$. (**C**) WT mice that had undergone splenectomy were treated as in **A**; after 6 days, percent Ter119$^+$CD45$^-$ cells in BM and PBMCs was assessed. Mean ± SD is shown. Data are representative of 2 independently repeated experiments with at least 3 mice per group.

Macrophages are essential for HVEM-mediated Epo production. We next investigated the cellular and molecular mechanisms underlying HVEM signal–mediated Epo production. Because HVEM is broadly expressed in both hematopoietic and nonhematopoietic organs, including the kidney (28), we first addressed which subsets among HVEM-expressing cells are necessary for Epo upregulation. We generated hematopoietic chimeric mice by transferring WT or *Hvem*$^{-/-}$ BM cells into lethally irradiated WT or *Hvem*$^{-/-}$ mice. When recipient mice were reconstituted with *Hvem*$^{-/-}$ BM cells, serum Epo upregulation and erythropoiesis in response to HM3.30 was completely abrogated, regardless of recipient type (Figure 5A and Supplemental Figure 3A). On the other hand, in recipients of WT BM cells, HM3.30 administration induced erythropoiesis even in *Hvem*$^{-/-}$ recipient mice. These data demonstrate that expression of HVEM on BM-derived hematopoietic cells is necessary and sufficient for HVEM-mediated Epo production and erythropoiesis.

Next, we sought to identify which population among hematopoietic cells is responsible for HVEM-mediated erythropoiesis. In *Rag*$^{-/-}$ mice, which lack mature T and B lymphocytes, HM3.30 injection still induced significant expansion of erythroid lineage cells (Supplemental Figure 4A). In mice treated with anti-NK1.1 mAb to deplete NK cells, the effect of HM3.30 also remained intact (Supplemental Figure 4B). Mice in which more than 95% of granulocytes were depleted by administration of anti–Gr-1 mAb also responded to HM3.30 treatment (Supplemental Figure 4, C and D). These results indicate that T cells, B cells, NK cells, and granulocytes are not necessary for HVEM-mediated erythropoiesis.

It was noted that HM3.30 administration induced a mild increase of F4/80$^+$ macrophages concomitantly with the enhanced erythropoiesis (Figure 1B). In addition, we found that almost 100% of F4/80$^+$ macrophages constitutively expressed HVEM on their cell surface (Supplemental Figure 5). Therefore, we next examined the role of macrophages in HVEM-mediated erythropoiesis. When mice were treated with clodronate liposomes, a reagent that selectively depletes F4/80$^+$ phagocytic macrophages (29, 30), upregulation of Epo production and expansion of Ter119$^+$CD45$^-$ erythrocytes by HM3.30 injection were completely abrogated (Figure 5B and Supplemental Figure 3B). These results indicate that macrophages are essential for HVEM-mediated Epo production and erythropoiesis.

HVEM stimulates Epo production via NO and HIF-1α upregulation in the kidney. It has been reported that HVEM signals facilitate NO production in macrophages (24). It is also known that NO stimulates HIF activity via (a) stabilization of HIF-α protein through inhibition of PHD activity and induction of HIF-1α S-nitrosylation and (b) enhancement of HIF-α synthesis mediated by PI3K and MAPK activation (15–18). Therefore, we hypothesized that HVEM signals stimulate Epo production via induction of macrophage-derived NO and subsequent upregulation of HIF-α. To address this possibility, we first assessed NO production by macrophages in HM3.30-treated mice and found a significant increase of

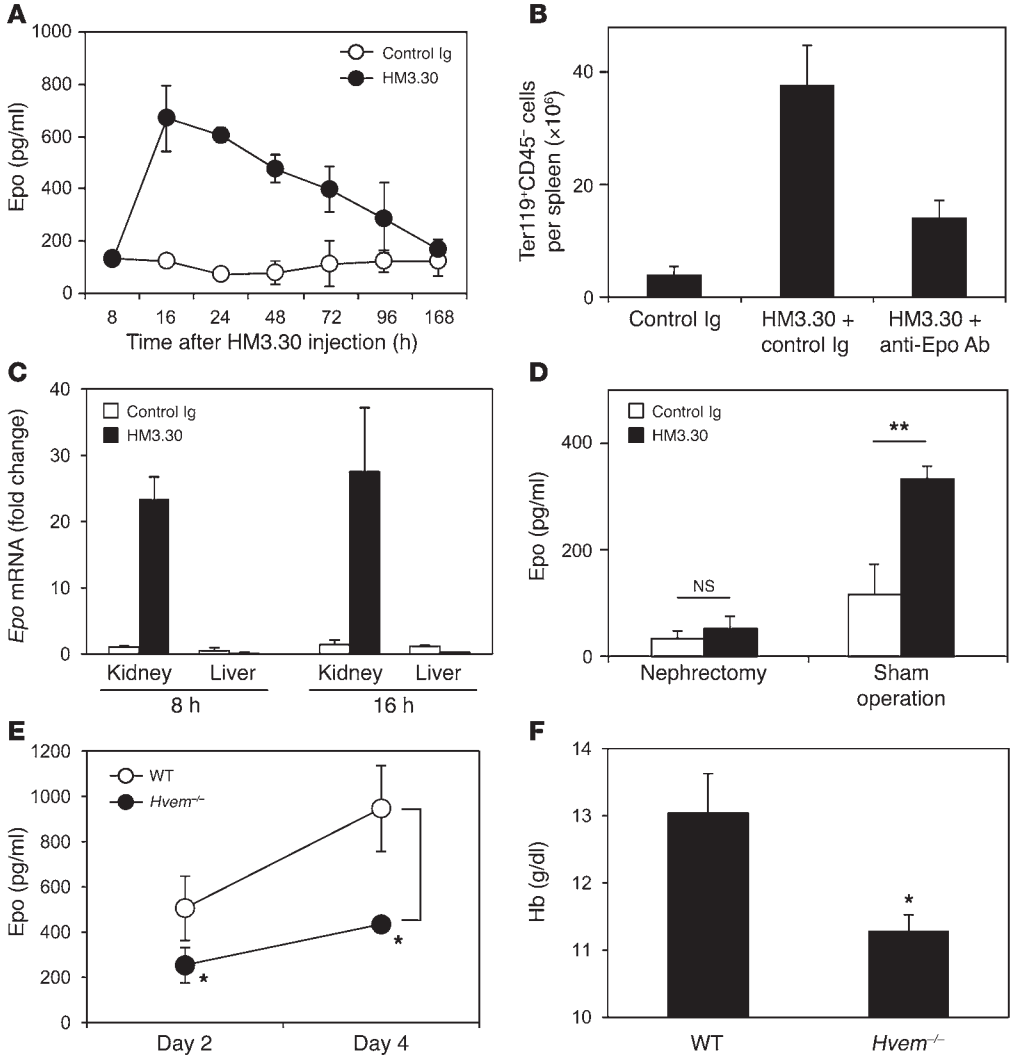

Figure 4

HVEM stimulation promotes erythropoiesis via renal Epo production. (**A**) WT mice were injected i.p. with 150 μg control Ig or HM3.30. Serum Epo levels were measured at the indicated time points. (**B**) WT mice were first injected i.p. with 150 μg control Ig or anti-Epo neutralizing mAb before receiving treatment as in **A** 4 hours later. After 4 days, absolute number of Ter119$^+$CD45$^-$ cells per spleen was measured by flow cytometry. (**C**) WT mice were treated as in **A**. After 8 and 16 hours, RNA was isolated from the kidney and liver, and analyzed by real-time PCR for the expression of *Epo*. PCR products were normalized to the expression of 18S and shown as fold change compared to the control. (**D**) WT mice received bilateral nephrectomy or sham operation and, 1 hour after surgery, were treated as in **A** (except that injections were i.v.). After 16 hours, serum Epo level was measured. (**E** and **F**) WT and *Hvem*$^{-/-}$ mice were injected i.v. with 3 mg/kg cisplatin daily from day 0 to day 3. (**E**) On days 2 and 4, serum Epo level was measured. (**F**) On day 8, peripheral blood Hb level was measured. Data represent mean ± SEM ($n \geq 4$ mice per group). $^{**}P < 0.01$; $^{*}P < 0.05$.

NO production as early as 5–10 hours after treatment (Figure 6A). On the other hand, we could not detect an increase of serum NO level in HM3.30-treated mice (data not shown), which suggests that HVEM-mediated NO upregulation appears to be a tissue-associated, not a systemic, event. Since the kidney was indispensable for HVEM-mediated Epo production (Figure 4D), we next determined expression of iNOS, an enzyme responsible for NO synthesis in macrophages (31), in the kidney of HM3.30-treated mice. We found that HM3.30 treatment upregulated *iNOS* mRNA expression in the kidney by 8.6-fold, while this response was completely abrogated by depletion of macrophages (Figure 6B). A significant increase of iNOS-expressing macrophages, but not granulocytes, in the kidney of HM3.30-treated mice was also confirmed by flow cytometric analysis (Figure 6C). These results indicate a crucial role of renal macrophages as NO producers in response to HVEM stimulation.

Next, we examined HIF-α levels in the kidney of HM3.30-treated mice. While there was no significant change in renal mRNA levels of *Hif1*α and *Hif2*α, HM3.30 treatment increased HIF-1α protein expression in nuclear extract of the kidneys (Figure 6, D and E). Protein expression of HIF-2α was not detected in HM3.30-treated and control mice; this was not the result of technical failure, since strong HIF-2α expression was detected in the cells treated with $CoCl_2$, a reagent that mimics hypoxia

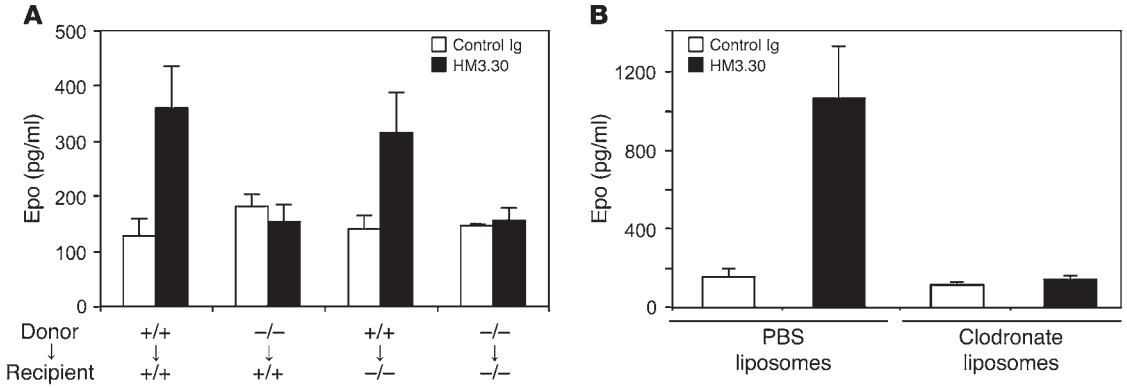

Figure 5

Essential role of macrophage in HVEM-mediated erythropoiesis. (**A**) BM chimeric mice were established by transferring 5×10^6 donor BM cells derived from WT or *Hvem*$^{-/-}$ mice into lethally irradiated WT or *Hvem*$^{-/-}$ recipient mice. 6 weeks later, chimeric mice were injected i.p. with 150 μg control Ig or HM3.30. After 4 days, serum Epo levels were measured. (**B**) WT C57BL/6 mice were injected i.v. with 200 μl clodronate liposomes or control PBS liposomes and, 1 day later, treated i.p. with 150 μg HM3.30 or control Ig. After 4 days, serum Epo levels were measured. Data represent mean ± SD ($n \geq 3$ mice per group).

conditions. These results thus suggest that HVEM signal upregulates HIF-1α through posttranscriptional mechanisms. In addition, immunohistochemical staining of the kidney revealed that HM3.30 treatment enhanced HIF-1α expression in the nuclei of renal tubular and peritubular interstitial cells in the cortex-medulla junction area (Figure 6F and Supplemental Figure 6). Taken together, these observations suggest that Epo production by HVEM stimulation is associated with macrophage-derived NO production and HIF-1α upregulation in the kidneys.

HIF-1α promotes transcription of various genes, including *VEGF* and phosphoglycerate kinase 1 (*PGK1*), as well as *EPO* (4, 10). We found that expression of *Vegf* and *Pgk1* in the kidney was also strikingly enhanced by HM3.30 treatment, and these responses were completely attenuated by depletion of macrophages by clodronate liposome administration (Supplemental Figure 7). Enhancement of *Vegf* and *Pgk1* gene expression was undetected in the liver, as was hepatic *Epo* expression in response to HM3.30 treatment (Figure 4C). These results suggest that HVEM signal upregulates HIF-1α and its downstream gene expressions in selected organs, including the kidney.

Finally, to address a causative role of NO in HVEM-mediated Epo upregulation, we attenuated NO production by G-nitro-L-arginine-methyl ester (L-NAME), a pharmacological inhibitor of NOS, or by genetic ablation of *iNOS*. In vivo treatment with L-NAME inhibited reticulocyte percentage significantly and reduced renal Epo expression in HM3.30-treated mice (Figure 7, A and B). In addition, *iNOS*$^{-/-}$ mice exhibited markedly — but not fully — attenuated renal Epo expression in response to HM3.30 treatment (Figure 7C). Although a potential contribution of iNOS/NO-independent mechanisms remains possible, our data indicate that NO production mediated by iNOS activity plays a crucial role in HVEM-mediated Epo upregulation and erythropoiesis.

HVEM stimulation is not associated with systemic or local hypoxia. The erythropoietic effect of HM3.30 was observed under normoxic experimental conditions. In order to fully exclude the possibility that HM3.30 treatment induces hypoxia systemically or locally in the kidneys, secondarily increasing HIF-1α–dependent Epo production and erythropoiesis, we first performed blood gas analysis. There was no significant differences in the arterial partial pressure of oxygen (PO_2) level between mice treated with control Ig or HM3.30 (Supplemental Figure 8A). Next, we examined the possibility that HM3.30 causes local hypoxia in the kidney. The level of renal blood flow was not significantly changed by HM3.30 treatment (Supplemental Figure 8B). In addition, direct and real-time measurement of tissue PO_2 level in the kidney by a fluorescent-quenching optical probe detected no significant changes in renal tissue PO_2 level after HM3.30 treatment (Supplemental Figure 8C). These results together indicate that HVEM stimulation does not induce systemic or renal hypoxia, which supports a role of HVEM signaling to trigger NO/HIF-1α–mediated Epo upregulation under nonhypoxic conditions.

Discussion

Although HVEM was originally identified as a cellular receptor mediating the entry of herpes simplex virus (28), subsequent studies identified its cosignaling functions in mature immune cells (22, 23). The current study revealed a third biological function of HVEM as a regulator of renal Epo production and erythropoiesis. Induction of HVEM signals by administration of agonistic mAb triggered NO production from renal macrophages and promoted HIF-1α activity in the kidney. Consequently, renal Epo production was elevated, and the expansion and differentiation of erythroid progenitor cells was facilitated. On the other hand, *Hvem*$^{-/-}$ mice showed repressed Epo production in response to erythropoietic stress and displayed aggravated anemia. Thus, our findings demonstrated what we believe to be a novel function of HVEM in the regulation of HIF and erythropoiesis.

HIF is the master regulator of adaptive responses to oxygen deprivation, including angiogenesis, erythropoiesis, vasomotor control, energy metabolism, and decisions regulating survival and death (4, 10). Although HIF activity is regulated by oxygen sensors, such as PHD and FIH, recent advances indicate that oxygen-independent factors also make use of the HIF-mediated gene regulatory system (10, 11). For instance, inflammatory mediators under infectious conditions, such as LPS and cytokines, upregulate HIF activity regardless of hypoxic stress and promote HIF-driven gene expression, which in turn potentiates antipathogenic effects of innate immune cells (32, 33). Here, we demonstrated

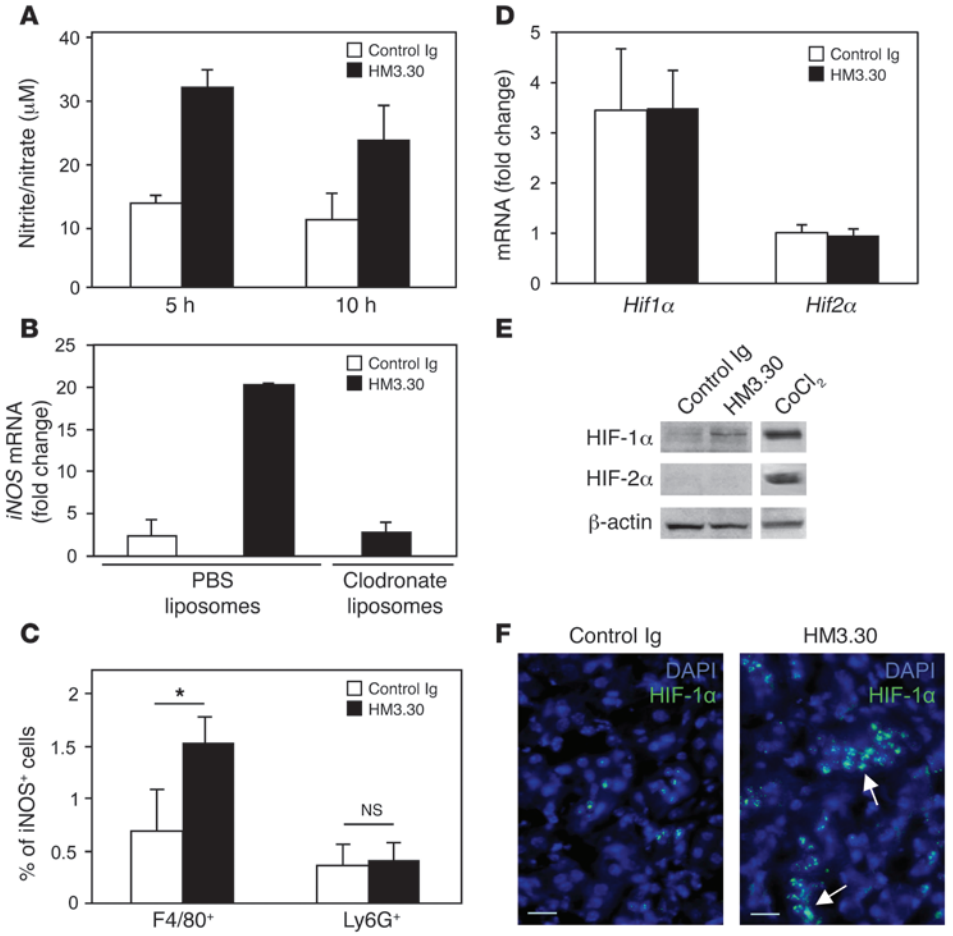

Figure 6

HM3.30-induced Epo production is associated with NO and HIF-1α upregulation in the kidney. WT mice were injected i.p. with 150 μg control Ig or HM3.30. (**A**) After 5 and 10 hours, splenic macrophages were harvested and incubated in vitro for 48 hours. Nitrite/nitrate levels in the supernatants were measured. (**B**) Mice were injected i.v. with 200 μl clodronate liposomes or control PBS liposomes 1 day before HM3.30 or control Ig treatment. After 8 hours, *iNOS* mRNA level in the kidney was examined by real-time PCR. (**C**) After 4 hours, kidneys were harvested and processed to generate cell suspension, followed by flow cytometric analysis of percent iNOS$^+$ cells in F4/80$^+$CD45$^+$ macrophage or Ly6G$^+$CD45$^+$ granulocyte populations. *$P < 0.05$. (**D**) After 4 hours, kidney expressions of *Hif1α* and *Hif2α* mRNA were assessed by real-time PCR. (**E**) After 4 hours, HIF-1α and HIF-2α expression on kidney-derived nuclear extracts was analyzed by Western blot. Nuclear extracts from Hepa1-6 tumor cells treated with $CoCl_2$ (150 μM) for 4 hours were used as positive control. (**F**) After 2 hours, kidneys were harvested and stained with anti–HIF-1α Ab followed by detection with Alexa Fluor 488–conjugated secondary Ab (green). Cell nuclei were counterstained with DAPI (blue). Arrows indicate positive staining of HIF-1α. Original magnification, ×400. Scale bars: 20 μm. Data represent mean ± SD ($n = 3$ per group).

another example of hypoxia-independent HIF regulation mediated by HVEM signaling through NO production by renal macrophages. Although it was reported that enhanced NO expression could stimulate Epo production by decreasing relative blood blow to the kidney (34), this mechanism was not responsible for the effects observed in our model, as no marked change in renal blood flow was detected in HM3.30-treated mice. In addition, direct measurement of kidney tissue PO_2 level also indicated that HVEM-mediated HIF-1α/Epo regulation is a mechanism operating under normoxic conditions.

Our results in experiments attenuating NO activities and depleting macrophages are indicative of an essential role of macrophage-associated NO production in HVEM-mediated erythropoiesis. The stimulatory role of NO in Epo production was previously reported in models using pharmacological methods to increase NO production. For instance, inclusion of S-nitroso-*N*-acetyl-DL-penicillamine, an NO donor, to primary rat dorsal root ganglion cultures upregulates Epo transcription in glial cells in a HIF-1α–dependent fashion (35). In addition, daily injections of sodium nitroprusside, a generator of NO, significantly increased serum Epo levels (36). Interestingly, our results demonstrated a dispensable role of granulocytes in iNOS expression and erythropoiesis mediated by HVEM signals, in spite of the potential of HVEM signaling to stimulate NO production in granulocytes as well as macrophages (24). Although a precise mechanism remains to be explored, this result could be explained by distinct thresholds between macrophages and granulocytes in response to HVEM signaling. Indeed, a previous study reported that the HVEM signal strength required for NO production in macrophages is 10 times less than that required in granulocytes (24). Excepting the enhanced NO production, HM3.30 treatment changed neither the number nor the M1/M2 marker expression pattern of renal macrophages (data not shown). Furthermore, HVEM stimulation did not affect expressions of *Epo*, *Vegf*, and *Pgk1* genes in the liver. Collectively, our present findings suggest that HVEM signaling triggered by HM3.30 selectively facilitates NO production in renal macrophages. Molecular mechanisms of this selectivity need to be explored in future studies.

Our results demonstrated that HVEM stimulation upregulated HIF-1α expression in both renal tubular and peritubular interstitial cells. Although predominant Epo producers under hypoxic conditions are interstitial cells in the kidney (37–39), it has also been shown that renal tubular cells have the potential to produce Epo under certain experimental conditions. For instance, ablation of GATA repressor functions triggers Epo expression in renal tubular cells under normoxia (40). In addition, in renal cell carcinoma patients with the complication of polycythemia, EPO expression is detected in the neoplastic tubular epithelium (41). At the in vitro culture level, it was also reported that macrophage-derived NO induces HIF-1α expression in coincubated kidney tubular LLC-PK1 cells (42). Thus,

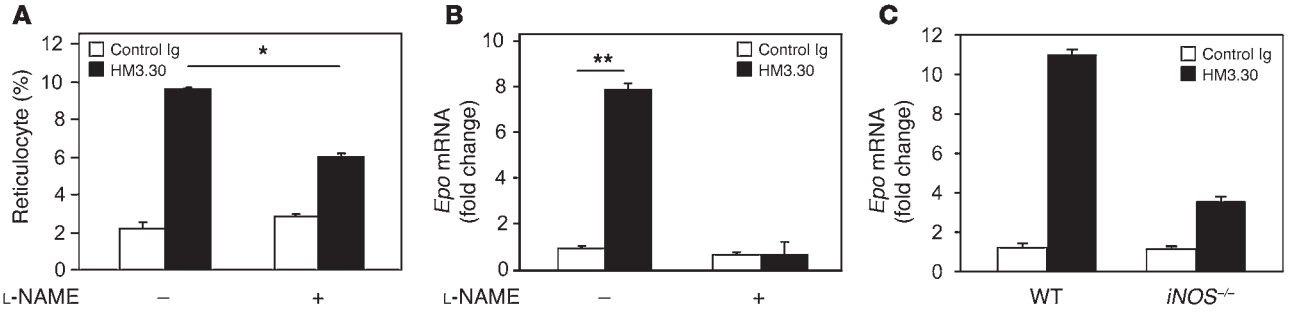

Figure 7

NO is essential for HM3.30-mediated Epo production. (**A** and **B**) WT C57BL/6 mice were injected i.p. with 150 μg control Ig or HM3.30 on day 0. Mice were subsequently treated i.p. with or without 100 mg/kg L-NAME every 24 hours for 4 days (n = 3 per group). (**A**) Percent reticulocytes was assessed by flow cytometry on day 4. (**B**) RNA was extracted from the kidneys on day 1, and *Epo* mRNA expression level was determined by real-time PCR. (**C**) WT or *iNOS*$^{-/-}$ mice were injected i.p. with 150 μg control Ig or HM3.30. After 4 hours, RNA was isolated from the kidneys, and *Epo* mRNA expression was assessed by real-time PCR. Mean ± SEM are shown. *P < 0.01; **P < 0.001.

we postulate that HVEM-mediated NO production in renal macrophages induces HIF-1α and Epo expression in adjacent tubular cells as well as interstitial cells under normoxic conditions.

We detected enhanced protein expression of HIF-1α, but not HIF-2α, in the kidneys of HM3.30-treated mice. Although this finding seems inconsistent with previous studies that suggested an important role of HIF-2α in Epo production in response to hypoxic stimuli (43–45), it is necessary to consider that the effect of HVEM operates under normoxic conditions. There is compelling evidence that HIF-1α can be upregulated by various stimuli other than hypoxia (12–18). In addition, recent studies directly revealed that HIF-1α contributes to NO-mediated Epo production in normoxic condition (35). Nevertheless, we cannot fully exclude the possibility that weak expression of HIF-2α, which was below the detection limit in our immunoblotting methods, may also contribute to Epo upregulation in our model. Further studies are necessary to address more precise roles of HIF-1α or HIF-2α in HVEM-mediated Epo upregulation.

Although NO-dependent HIF-1α/Epo upregulation plays an essential role in HVEM-mediated erythropoiesis, our results also suggest the possible involvement of other mechanisms. First, ablation of NO activity using *iNOS*$^{-/-}$ mice significantly inhibited HVEM-mediated erythropoiesis, but resulted in incomplete attenuation. Thus, NO-independent mechanisms may play some role in the effects of HVEM. Since HVEM is a potent inducer of the NF-κB signaling pathway (20–22), it is possible that HVEM upregulates HIF-1α through an NF-κB–dependent mechanism (12). Second, treatment with anti-Epo neutralizing Ab resulted in incomplete attenuation of erythropoiesis induced by HVEM. Although dose insufficiency of anti-Epo Ab could be a potential cause, it is also possible that HVEM stimulates erythropoiesis through Epo-independent mechanisms. For instance, HVEM may have direct actions on hematopoietic stem cells or myeloid stem cells to promote their potential to differentiate into an erythroid lineage, similar to those observed in Chuvash polycythemia (46). In addition, a recent study indicated that HIF-1α enhanced the effect of glucocorticoids to promote proliferation of Epo-insensitive erythroid burst-forming unit (BFU-E) progenitors, which also suggests the possibility that HVEM directly affects BFU-E cells to promote erythropoiesis through HIF-1α (47). In this regard, it should be noted that HVEM was highly expressed on hematopoietic stem cells and progenitor cells (data not shown).

The potential of HVEM signaling to facilitate endogenous Epo production suggests that supplementing HVEM signal can be applied to therapeutic approaches for Epo-responsive diseases, including anemia. Although recombinant EPO and its derivatives have achieved enormous success in treating more than 1,000,000 patients with anemia, these erythropoiesis-stimulating agents (ESAs) still have safety concerns and shortcomings worthy of improvement. It has been revealed that ESA administration increases the risk of thromboembolic events and shortens the survival of cancer patients (48–51). Accordingly, the recent guideline summarized by the American Society of Hematology and the American Society of Clinical Oncology recommends that ESAs should be administered at the lowest dose possible and should increase Hb to the lowest concentration possible to avoid transfusions in cancer patients receiving concurrent chemotherapy (52). Although precise mechanisms of the adverse effects of ESAs have yet to be fully elucidated, nonphysiological pharmacokinetics of exogenously injected recombinant EPO associated with its short half-life may be responsible, at least in part (52, 53). Administration of agonistic anti-HVEM mAb, on the other hand, induced endogenous Epo upregulation with a relatively long half-life (approximately 48–72 hours; Figure 4A). Thus, despite the need to proceed with caution, as with other ESAs, stimulation of HVEM signaling may create therapeutic opportunities for Epo-responsive diseases.

Methods

Mice, Abs, and reagents. Unless otherwise indicated, age-matched, 6- to 8-week-old female C57BL/6 mice (National Cancer Institute, NIH) were used in all experiments. *iNOS*$^{-/-}$ and *Rag*$^{-/-}$ mice were purchased from The Jackson Laboratory. *Hvem*$^{-/-}$ mice were generated as previously described (25). Agonistic anti-mouse HVEM mAb (clone HM3.30, hamster IgG) and antagonistic anti-mouse HVEM mAb (clone LBH1, hamster IgG) were generated in our laboratory (25). Anti-mouse Epo neutralizing mAb and ELISA kit for mouse Epo were purchased from R&D Systems. Fluorochrome-conjugated Abs for flow cytometry were purchased from BD Biosciences or eBioscience. BrdU Flow kit was purchased from BD Biosciences. New methylene blue and thiazole orange for reticulocyte staining were purchased from Sigma-Aldrich and FLUKA, respectively. L-NAME and a nitrite/nitrate assay kit were purchased from Cayman Chemical. Quantichrom kit to measure peripheral blood Hb level was purchased from BioAssay Systems.

CFU-E assay. BM cells were harvested by flushing the femur and tibia of the mice and were plated on MethoCult media for CFU-E assay (M3334, Stem Cell Technologies) according to the manufacturer's instructions. After 2 days, the number of colonies was estimated by staining plates with benzidine.

Splenectomy and nephrectomy. Mice were anesthetized by injection of tribromoethanol (Sigma-Aldrich). For splenectomy, a transverse incision was made on the left lower back to expose the spleen. The gastrosplenic ligament was cut, the splenic blood vessels were tied off with silk suture, and the spleen was removed. The incisions were closed with sutures on the body wall followed by wound clips on the skin. After 2 days, the mice were used for mAb injection experiments. For bilateral nephrectomy, mouse kidneys were exposed through flank incisions. The renal pedicles were ligated with sutures and cut distal to the suture. The incisions were closed in a single layer with wound clips. The sham surgery group underwent similar incisions and exposure of kidneys, followed by closing of the incisions. When the mice recovered from anesthesia (typically 1 hour later), they were injected with mAb. After 16 hours, the mice were euthanized for serum sampling.

Real-time PCR. At the indicated time after mAb treatment, total RNA was isolated from the kidneys and liver by homogenization with TRIzol Reagent (Invitrogen). cDNA was synthesized using SuperScript II reverse transcriptase (Invitrogen). Real-time PCR was carried out in a LightCycler (Roche Applied Science) using RT2 Real-Time SYBR green PCR master mix (SA Biosciences). Real-time PCR conditions were as follows: initial denaturation at 95°C for 10 minutes; followed by 40 cycles of denaturation at 95°C for 10 seconds, annealing/detection at 57°C for 30 seconds, and extension at 72°C for 15 seconds. The primers used in this study were as follows: *18S* sense, 5′-TTAAGAGGGACGGCCGGGGG-3′; *18S* antisense, 5′-GCATCGCCAGTCGGCATCGT-3′; *Epo* sense, 5′-GGGTGCCCGAACGTCCCAC-3′; *Epo* antisense, 5′-AGATGAGGCGTGGGGGAGCA-3′; *Hif1*α sense, 5′-TCTGGATGCCGGTGGTCTAG-3′; *Hif1*α antisense, 5′-TGCAGTGAAGCACCTTCCAC-3′; *Hif2*α sense, 5′-TCAGTGCGAACATGGCCCCCGA-3′; *Hif2*α antisense, 5′-AGCACTGTGGCGGGAACCCA-3′; *iNOS* sense, 5′-TCACCTTCGAGGGCAGCCGA-3′; *iNOS* antisense, 5′-ACCCAGTAGCTGCCGCTCTCAT-3′; *Vegf* sense, 5′-GTCCCATGAAGTGATCAAGTTC-3′; *Vegf* antisense, 5′-ATCCGCATGATCTGCATGGTG-3′; *Pgk1* sense, 5′-GCTGGATGGGCTTGGACTGTGGTA-3′; *Pgk1* antisense, 5′-AGGAGCACAGGAACCAAAGGCAGG-3′. Specificity of the primers was verified by a size of PCR product in agarose gel electrophoresis and by melting curve analysis. Gene expression was normalized to *18S*, and fold changes were calculated using ΔΔCt method by comparing expression levels in Ab-treated mice with those in control Ig–treated mice.

Generation of BM chimeric mice. To generate BM chimeric mice, the recipient mice were exposed to 6 Gy irradiation twice at 4-hour intervals, then transferred i.v. with 5×10^6 donor BM cells within 1 hour of the final irradiation. Mice were allowed to recover from BM transfer for at least 6 weeks before being used for further experiments.

Macrophage depletion in vivo. 200 μl clodronate liposomes or control PBS liposomes were administrated i.v. into mice. Clodronate was a gift from Roche Diagnostics. Clodronate was capsulated in liposomes as described previously (29).

Western blot analysis. Mouse kidneys were homogenized in a tissue grinder and lysed by hypotonic lysis buffer (10 mM Tris-HCl, pH 7.5; 1.0 mM $MgCl_2$; 10 mM KCl; 5 mM EDTA; 1 mM EGTA; 1.0 mM dithiothreitol; 1.0 mM Na_3VO_4; and cocktails of protease inhibitors). The nuclear fractions were separated as previously reported (54), and equal quantities of proteins from the nuclear fraction lysates (approximately 50 μg) were loaded on 4%–12% Bis-Tris NuPage denaturing gel (Invitrogen) for electrophoresis. Proteins were transferred onto nitrocellulose membrane, probed with a rabbit polyclonal anti–HIF-1α or anti–HIF-2α Ab (Novus Biologicals), which recognizes HIF-α/β dimers as well as HIF-α monomer, and exposed to a WesternBreeze Chemiluminescent detection kit (Invitrogen). Equal loading of the proteins was confirmed by reprobing of the blot with an anti–β-actin Ab (Cell Signaling Technology).

Immunofluorescence staining. Mouse kidneys were snap-frozen in OCT compound and cut into 5-μm-thick sections, followed by mounting on gelatin-coated slides and fixation with aceton at –20°C for 10 minutes. After washing with PBS, the sections were incubated overnight with rabbit anti–HIF-1α Ab at 4°C. Staining of HIF-1α was detected by a 2-layer approach by incubating first with FITC-labeled anti-rabbit IgG and then with Alexa Fluor 488–conjugated anti-FITC Ab, both at room temperature for 1 hour. Cell nuclei were counterstained with DAPI. Images were acquired using a Nikon Eclipse E600 fluorescence microscope (Nikon Instruments Inc.) equipped with a SPOT digital camera and imaging software.

Statistics. Statistical analyses used unpaired 2-tailed Student's *t* test. Differences were considered significant at P values less than 0.05.

Study approval. All animal experiments were approved by the Animal Care and Use Committee of the Johns Hopkins University or the University of Maryland Baltimore.

Acknowledgments

We thank Curt Civin for critical comments on these studies and Mathew M. Augustine for technical help in some experiments. This study was supported by NIH grant HL088954 (to K. Tamada).

Received for publication January 31, 2011, and accepted in revised form October 11, 2011.

Address correspondence to: Koji Tamada, University of Maryland School of Medicine, 655 W. Baltimore St., Bressler Research Building, Rm 9-051, Baltimore, Maryland 21201, USA. Phone: 410.328.5114; Fax: 410.328.6559; E-mail:ktamada@som.umaryland.edu.

1. Fisher JW. Erythropoietin: physiology and pharmacology update. *Exp Biol Med (Maywood)*. 2003; 228(1):1–14.
2. Jelkmann W. Molecular biology of erythropoietin. *Intern Med*. 2004;43(8):649–659.
3. Fandrey J. Oxygen-dependent and tissue-specific regulation of erythropoietin gene expression. *Am J Physiol Regul Integr Comp Physiol*. 2004;286(6):R977–R988.
4. Schofield CJ, Ratcliffe PJ. Oxygen sensing by HIF hydroxylases. *Nat Rev Mol Cell Biol*. 2004; 5(5):343–354.
5. Webb JD, Coleman ML, Pugh CW. Hypoxia, hypoxia-inducible factors (HIF), HIF hydroxylases and oxygen sensing. *Cell Mol Life Sci*. 2009;66(22):3539–3554.
6. Ivan M, et al. HIFalpha targeted for VHL-mediated destruction by proline hydroxylation: implications for O2 sensing. *Science*. 2001;292(5516):464–468.
7. Jaakkola P, et al. Targeting of HIF-alpha to the von Hippel-Lindau ubiquitylation complex by O2-regulated prolyl hydroxylation. *Science*. 2001; 292(5516):468–472.
8. Yu F, White SB, Zhao Q, Lee FS. HIF-1alpha binding to VHL is regulated by stimulus-sensitive proline hydroxylation. *Proc Natl Acad Sci U S A*. 2001; 98(17):9630–9635.
9. Mahon PC, Hirota K, Semenza GL. FIH-1: a novel protein that interacts with HIF-1alpha and VHL to mediate repression of HIF-1 transcriptional activity. *Genes Dev*. 2001;15(20):2675–2686.
10. Semenza GL. Targeting HIF-1 for cancer therapy. *Nat Rev Cancer*. 2003;3(10):721–732.
11. Dehne N, Brune B. HIF-1 in the inflammatory microenvironment. *Exp Cell Res*. 2009;315(11):1791–1797.
12. Rius J, et al. NF-kappaB links innate immunity to the hypoxic response through transcriptional regulation of HIF-1alpha. *Nature*. 2008;453(7196):807–811.
13. Zhou J, Brune B. Cytokines and hormones in the regulation of hypoxia inducible factor-1alpha (HIF-1alpha). *Cardiovasc Hematol Agents Med Chem*. 2006; 4(3):189–197.
14. Huang LE, Bunn HF. Hypoxia-inducible factor and its biomedical relevance. *J Biol Chem*. 2003; 278(22):19575–19578.
15. Berchner-Pfannschmidt U, Tug S, Kirsch M, Fandrey J. Oxygen-sensing under the influence of nitric oxide. *Cell Signal*. 2010;22(3):349–356.
16. Brune B, Zhou J. Nitric oxide and superoxide: interference with hypoxic signaling. *Cardiovasc Res*. 2007; 75(2):275–282.
17. Li F, et al. Regulation of HIF-1alpha stability through S-nitrosylation. *Mol Cell*. 2007;26(1):63–74.

18. Kasuno K, et al. Nitric oxide induces hypoxia-inducible factor 1 activation that is dependent on MAPK and phosphatidylinositol 3-kinase signaling. *J Biol Chem*. 2004;279(4):2550–2558.
19. Murphy TL, Murphy KM. Slow down and survive: Enigmatic immunoregulation by BTLA and HVEM. *Annu Rev Immunol*. 2010;28:389–411.
20. Marsters SA, Ayres TM, Skubatch M, Gray CL, Rothe M, Ashkenazi A. Herpesvirus entry mediator, a member of the tumor necrosis factor receptor (TNFR) family, interacts with members of the TNFR-associated factor family and activates the transcription factors NF-kappaB and AP-1. *J Biol Chem*. 1997;272(22):14029–14032.
21. Harrop JA, et al. Herpesvirus entry mediator ligand (HVEM-L), a novel ligand for HVEM/TR2, stimulates proliferation of T cells and inhibits HT29 cell growth. *J Biol Chem*. 1998;273(42):27548–27556.
22. Tamada K, et al. Modulation of T-cell-mediated immunity in tumor and graft-versus-host disease models through the LIGHT co-stimulatory pathway. *Nat Med*. 2000;6(3):283–289.
23. Tamada K, et al. LIGHT, a TNF-like molecule, costimulates T cell proliferation and is required for dendritic cell-mediated allogeneic T cell response. *J Immunol*. 2000;164(8):4105–4110.
24. Heo SK, et al. LIGHT enhances the bactericidal activity of human monocytes and neutrophils via HVEM. *J Leukoc Biol*. 2006;79(2):330–338.
25. Xu Y, et al. Selective targeting of the LIGHT-HVEM costimulatory system for the treatment of graft-versus-host disease. *Blood*. 2007;109(9):4097–4104.
26. Jelkmann W. Erythropoietin: structure, control of production, and function. *Physiol Rev*. 1992; 72(2):449–489.
27. Weidemann A, Johnson RS. Nonrenal regulation of EPO synthesis. *Kidney Int*. 2009;75(7):682–688.
28. Montgomery RI, Warner MS, Lum BJ, Spear PG. Herpes simplex virus-1 entry into cells mediated by a novel member of the TNF/NGF receptor family. *Cell*. 1996;87(3):427–436.
29. Van Rooijen N, Sanders A. Liposome mediated depletion of macrophages: mechanism of action, preparation of liposomes and applications. *J Immunol Methods*. 1994;174(1–2):83–93.
30. Zeisberger SM, Odermatt B, Marty C, Zehnder-Fjallman AH, Ballmer-Hofer K, Schwendener RA. Clodronate-liposome-mediated depletion of tumour-associated macrophages: a new and highly effective antiangiogenic therapy approach. *Br J Cancer*. 2006;95(3):272–281.
31. MacMicking J, Xie QW, Nathan C. Nitric oxide and macrophage function. *Annu Rev Immunol*. 1997; 15:323–350.
32. Nizet V, Johnson RS. Interdependence of hypoxic and innate immune responses. *Nat Rev Immunol*. 2009; 9(9):609–617.
33. Peyssonnaux C, et al. HIF-1alpha expression regulates the bactericidal capacity of phagocytes. *J Clin Invest*. 2005;115(7):1806–1815.
34. Boutin AT, et al. Epidermal sensing of oxygen is essential for systemic hypoxic response. *Cell*. 2008; 133(2):223–234.
35. Keswani SC, Bosch-Marce M, Reed N, Fischer A, Semenza GL, Hoke A. Nitric oxide prevents axonal degeneration by inducing HIF-1-dependent expression of erythropoietin. *Proc Natl Acad Sci U S A*. 2011;108(12):4986–4990.
36. Ohigashi T, Brookins J, Fisher JW. Interaction of nitric oxide and cyclic guanosine 3′,5′-monophosphate in erythropoietin production. *J Clin Invest*. 1993;92(3):1587–1591.
37. Lacombe C, et al. Peritubular cells are the site of erythropoietin synthesis in the murine hypoxic kidney. *J Clin Invest*. 1988;81(2):620–623.
38. Semenza GL, Koury ST, Nejfelt MK, Gearhart JD, Antonarakis SE. Cell-type-specific and hypoxia-inducible expression of the human erythropoietin gene in transgenic mice. *Proc Natl Acad Sci U S A*. 1991; 88(19):8725–8729.
39. Maxwell PH, et al. Identification of the renal erythropoietin-producing cells using transgenic mice. *Kidney Int*. 1993;44(5):1149–1162.
40. Obara N, Suzuki N, Kim K, Nagasawa T, Imagawa S, Yamamoto M. Repression via the GATA box is essential for tissue-specific erythropoietin gene expression. *Blood*. 2008;111(10):5223–5232.
41. Da Silva JL, et al. Tumor cells are the site of erythropoietin synthesis in human renal cancers associated with polycythemia. *Blood*. 1990;75(3):577–582.
42. Zhou J, Fandrey J, Schumann J, Tiegs G, Brune B. NO and TNF-alpha released from activated macrophages stabilize HIF-1alpha in resting tubular LLC-PK1 cells. *Am J Physiol Cell Physiol*. 2003; 284(2):C439–C446.
43. Scortegagna M, et al. HIF-2alpha regulates murine hematopoietic development in an erythropoietin-dependent manner. *Blood*. 2005;105(8):3133–3140.
44. Rankin EB, et al. Hypoxia-inducible factor-2 (HIF-2) regulates hepatic erythropoietin in vivo. *J Clin Invest*. 2007;117(4):1068–1077.
45. Kapitsinou PP, et al. Hepatic HIF-2 regulates erythropoietic responses to hypoxia in renal anemia. *Blood*. 2010;116(16):3039–3048.
46. Ang SO, et al. Disruption of oxygen homeostasis underlies congenital Chuvash polycythemia. *Nat Genet*. 2002;32(4):614–621.
47. Flygare J, Rayon Estrada V, Shin C, Gupta S, Lodish HF. HIF1alpha synergizes with glucocorticoids to promote BFU-E progenitor self-renewal. *Blood*. 2011;117(12):3435–3444.
48. Henke M, et al. Erythropoietin to treat head and neck cancer patients with anaemia undergoing radiotherapy: randomised, double-blind, placebo-controlled trial. *Lancet*. 2003;362(9392):1255–1260.
49. Leyland-Jones B, et al. Maintaining normal hemoglobin levels with epoetin alfa in mainly nonanemic patients with metastatic breast cancer receiving first-line chemotherapy: a survival study. *J Clin Oncol*. 2005;23(25):5960–5972.
50. Wright JR, et al. Randomized, double-blind, placebo-controlled trial of erythropoietin in non-small-cell lung cancer with disease-related anemia. *J Clin Oncol*. 2007;25(9):1027–1032.
51. Dicato M, Plawny L. Erythropoietin in cancer patients: pros and cons. *Curr Opin Oncol*. 2010; 22(4):307–311.
52. Rizzo JD, et al. American Society of Hematology/American Society of Clinical Oncology clinical practice guideline update on the use of epoetin and darbepoetin in adult patients with cancer. *Blood*. 2010;116(20):4045–4059.
53. Fishbane S. Recombinant human erythropoietin: has treatment reached its full potential? *Semin Dial*. 2006;19(1):1–4.
54. Zhao Y, et al. Activation of keratinocyte protein kinase C zeta in psoriasis plaques. *J Invest Dermatol*. 2008;128(9):2190–2197.